NASA TECHNICAL TRANSLATION NASA TT F-15,068

OPERATING EXPERIENCE OBTAINED WITH A 100-kW WIND POWER PLANT

U. Hütter

(NASA-TT-F-15068) OPERATING EXPERIENCE OBTAINED WITH A 100 kW WIND POWER PLANT (Kanner (Leo) Associates)

N73-29008

10A G3/03

Unclas 11522

Translation of "Betriebserfahrungen mit einer Windkraftanlage von 100 kW," Brennstoff-Wärme-Kraft, Vol. 16, 1964, pp. 333-340

Reproduced by
NATIONAL TECHNICAL
INFORMATION SERVICE
US Department of Commerce
Springfield, VA. 22151

NATIONAL AERONAUTICS AND SPACE ADMINISTRATION
WASHINGTON, D.C. 20546 AUGUST 1973

STANDARD TITLE PAGE

1. Report No.	2. Government Accession No.	3. Recipient's Catalog No.
NASA TT F-15,068		

4. Title and Subtitle	5. Report Date
OPERATING EXPERIENCE OBTAINED WITH A 100-kW WIND POWER PLANT	August 1973
	6. Performing Organization Code

7. Author(s)	8. Performing Organization Report No.
U. Hütter	
	10. Work Unit No.

9. Performing Organization Name and Address	11. Contract or Grant No.
Leo Kanner Associates, P.O. Box 5187, Redwood City, California 94063	NASw-2481
	13. Type of Report and Period Covered
	Translation
12. Sponsoring Agency Name and Address	14. Sponsoring Agency Code
National Aeronautics and Space Administration, Washington, D.C. 20546	

15. Supplementary Notes
Translation of "Betriebserfahrungen mit einer Windkraftanlage von 100 kW," Brennstoff-Wärme-Kraft, Vol. 16, 1964, p. 333-340

16. Abstract An excerpt is given from the report on experiments and experience associated with the wind power plant developed and constructed by the Studiengesellschaft Windkraft, Stuttgart, covering design data and those aspects which were decisive in its layout and the type of regulating provisions used, as well as results of the detailed operational tests. The regulating system and the automatic cut-in provisions permit the system to be connected automatically to the public power supply network on the basis of a specific program. Its performance is compared with that of the Andreau-Enfield-Cables power plant in Algeria, which weighed 4.5 times as much; the former is found to reach full power at much lower wind velocities than the latter. The various types of wind conditions considered in designing the power plant are described.

PRICES SUBJECT TO CHANGE

17. Key Words (Selected by Author(s))	18. Distribution Statement
	Unclassified - Unlimited

19. Security Classif. (of this report)	20. Security Classif. (of this page)	21. No. of Pages	22. Price
Unclassified	Unclassified	26	

OPERATING EXPERIENCE OBTAINED WITH A 100-kW WIND POWER PLANT*

U. Hütter
Society for the Study of Wind Power

Prior History

/333**

In order to clarify the question as to whether the utilization of wind energy is economically reasonable, the establishment of a Studiengesellschaft Windkraft e.V. [Society for the Study of Wind Power] was proposed on December 15, 1949, by H. Christaller, Energieversorgung Schwaben AG [Swabian Power Corporation], with the goal of producing a wind power plant of adequate size as a research device for science, industry and the energy system. A design competition was announced for a power plant which would achieve a nominal output of 100 kW at a wind velocity of about 8 m/s.

The design by Allgaier-Wergzeugbau GmbH [Allgäu Tool Production Corporation], Uhingen/Württemberg, was selected for execution; it was produced in this firm's Development Department, directed by U. Hütter. In order to implement this project, a "Wind Power Development Group" was established on January 1, 1955, which included seven West German public power utilities and five firms in the electrical machinery industry and fluid-dynamics machinery construction. The Federal Ministry of Economics, the Baden-Württemberg Ministry of Economics, the Lower Saxony Ministry of

---

*Excerpt from "Final Report on the Construction and Testing of a 100-kW Wind Power Plant at Stötten bei Geisslingen/Württemberg," June 12, 1963. Author and Scientific Director of Design and Testing: Prof. Dr. rer. techn. Ulrich Hütter, VDI Chair and Institute of Aircraft Construction at the Engineering College of Stuttgart. Responsible for operation of the plant and execution of the measurements: Ing. Sepp Armbrust.

**Numbers in the margin indicate pagination in the foreign text.

Economics and Transportation, and the Deutsche Forschungsgemeinschaft [German Research Society] participated in financing. Outstanding service in the implementation of this project and the execution of tests was rendered by Ministerial Council Dipl.-Ing. K. Hipp (Baden-Württemberg Ministry of Economics), Director Dipl.-Ing. M. Stegemann (deceased) (Hamburgische Electricitäts-Werke AG [Hamburg Electric Corporation]) and Dipl.-Ing. R. Clausnizer (Elektrizitäts-Versorgung Schwaben AG [Swabian Electric Power Supply Corporation]).

The final report which is now available allows reliable and conclusive answers to the question posed above.[1]

Technical Data

Figures 1 through 3 show the construction of the power plant, which has been operating in parallel with the public power supply in Stötten bei Geisslingen/Württemberg since 1959. Technical data are summarized in Tables 1-3. The following blade profiles were used:

Radius R of blade tips, m [sic]	Profile thickness in % blade width	Profile type
0,5	100	Circle
3,0	32	Göttingen 643
6,5	21	NACA 64_4 621
11,0	18	NACA 64_3 618
17,0	18	NACA 64_3 618

[Note: Commas in numerals are equivalent to decimal points.]

[1]The reader is also referred to article [1] in this regard.

Nominal speed for the turbine wheel (main shaft d in Figs. 2 and 3) was 42 rpm for the tests up to September 28, 1959 and 34 rpm for the tests conducted after November 20, 1959. The following speed ratios[2] ($R\omega/v_o$) were obtained at 34 rpm, referred to the blade tip, in parallel operation with the power supply system:

Net power to network kW	Speed ratio λ_a
90	≦ 6,7
64	8,1
40	8,8
20	⊛11,8
10	12,7
2	16,2
Idling at nom. rpm	18 – 22

TABLE 1. AERODYNAMIC DESIGN

Radius to blade tips (R)	17.0 m
Conical angle (ψ)	7.0°
Effective diameter of blade circle ($D = 2\,R\cos\Psi$)	33.76 m
Inclination of axis relative to horizontal (ϕ)	10.2°
Effective area swept by blades ($A_\varnothing = R\pi\cos^2\phi\cos\psi$)	872 m^2
Area of one blade projected on reference plane* (S)	12.62 m^2
Aspect ratio ($A = R^2/S$)	22.5
Area density of blade ($\Phi_r = 2S/A_\varnothing$)	2.91%
Height of axis of effective blade area above ground	24.2 m

*Plane of blade chords at 0.72 R.

[2] See also Fig. 7.

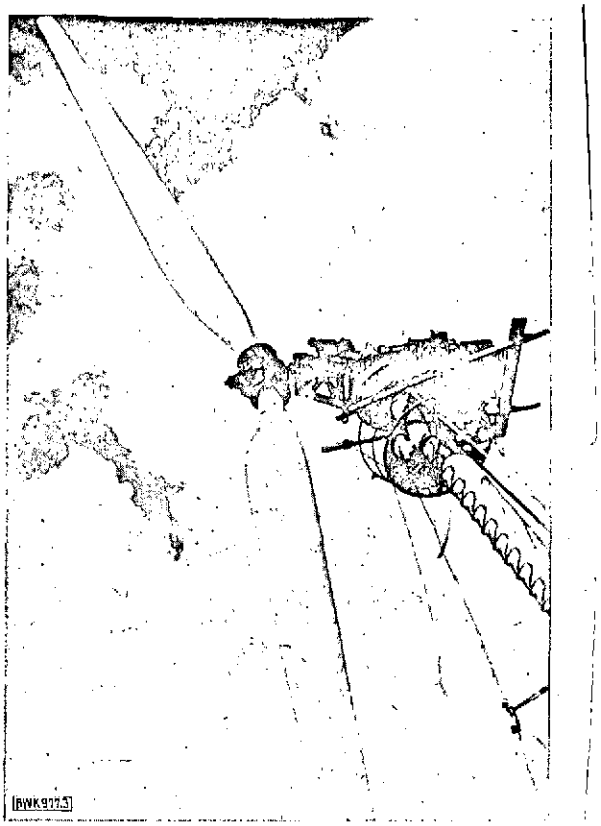

Fig. 1. View of the 100-kW test plant during final assembly.

Results of Energy Output Measurement in Routine Operation

G. Clausnizer has shown [2] that taking relatively short-term averages of wind velocity and power by summing wind paths and kWh outputs provide the most reliable indication of the relationship between the velocity of undisturbed homogeneous wind flow at the plane of rotation and the plant's actual power output. Such instantaneous-value measurements can also provide highly reliable information on the plant's instantaneous reaction to the velocity of undisturbed oncoming flow and on the energy output to be calculated from long-term averages of wind velocity.

The output of the wind power plant was measured on the basis of principles discussed in [2]. Two Tritschler IRG/ism pulsed recorders were available for this purpose, with a synchronous drive system for use as a time-measuring unit, and with master clock contacts. One instrument recorded energy output and produced a pulse to advance the recording strip 0.2 mm (unit of advance) for each 0.033 kWh, the fixed unit. In an analogous manner, the other instrument provided an advance pulse of the same magnitude after a wind path of 20 m (the fixed unit) had been covered. The time holes punched in the strips of the two instruments at intervals of 6 min were synchronized.

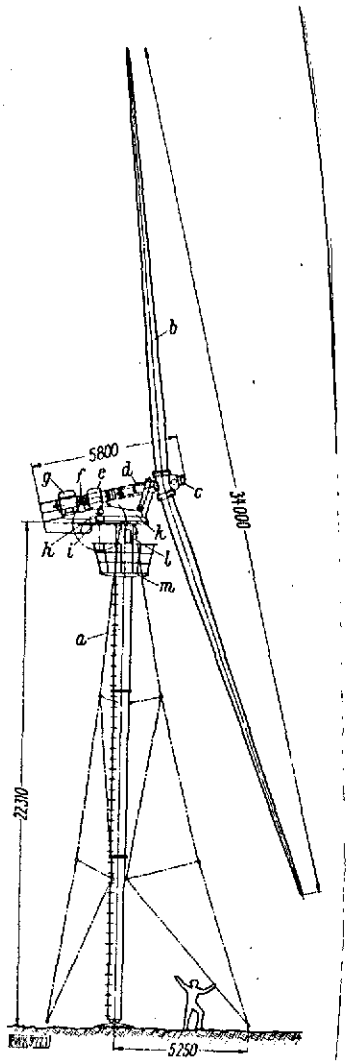

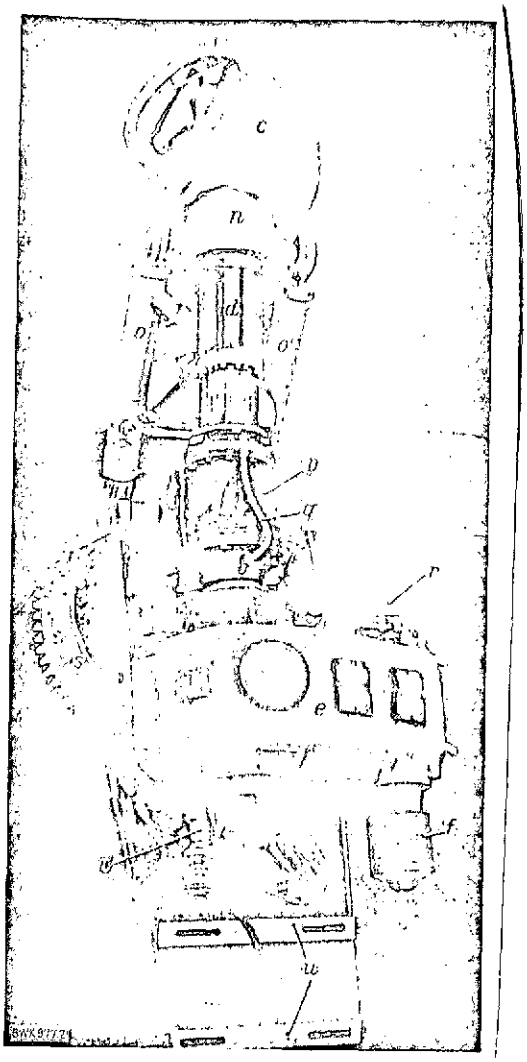

Figs. 2 and 3. Stötten 100-kW test plant of the Studiengesellschaft Windkraft.

Right; Machinery unit prior to installation.

Rotor area	900 m^2
Nominal speed	42 rpm
Speed ratio	
Idling	20
Under nominal load	10

a Tubular tower
b Fiberglass-reinforced plastic blade (semicardan blade suspension)
c Control spider and hub with extremely shallow flat roller bearings
d Main shaft with blade adjustment motor (hydraulic pistons, 7-10 technical atmospheres gauge oil pressure)
e Voith three-stage spur-gear transmission (1:35.8)
f V-belt drive
g Synchronous generator, 100 kW, 1500 rpm, 50 Hz, self-excited via magnetic amplifier and choke coils

[Continued on following page.]

Key to Figs. 2 and 3, cont'd.:

h Directional servomotor
i Directional servo gearbox
k Welded machinery platform, simultaneously serving as oil tank for control equipment
l Access to slipring unit (four power sliprings and 22 control sliprings)
m Mast platform
n Main shaft bearing
o Originally elastic shaft support
p Universal joint
q Flexible hydraulic line to blade servomotor
r Brake on high-speed shaft
s Worm gear ring for directional adjustment
t Main hydraulic pump
u Mounts for generator g

TABLE 2. TOWER DIMENSIONS

Height of attachment flange above ground	22.3 m
Diameter of guys (St [steel] 70.11)	50 mm
Distance of anchor bolts from tower axis	10.5 m
Diameter of circle of support	14.0 m
Foundation volume	about 29 m^3

		Diameter of pipe section	Wall thickness	Section length
Bottom section	mm	500	8	7570
Middle section	mm	550	8	7200
Top section	mm	600	8	7200

The fixed quantities for output were measured by a kWh meter which had been modified for this purpose -- with contact made after the production of a fixed quantity of energy. The wind pickup was a triple cup anemometer which tripped a contact after an adjustable wind path had been covered. The wind transmitter was located 41 m from the center of the tower, set up at a height of 18.2 m on a free-standing tower. In order to determine the relationship between wind velocity and power (wind path and kWh output), it was therefore necessary to convert all wind velocity data to the corresponding values for the height of the axis of the effective rotor area above the ground (24.2 m).

TABLE 3. WIND POWER PLANT WEIGHTS (IN METRIC TONS).

Guyed tubular tower:	
Tower tubing	2.76
Guys	1.52
Anchor plate, bolts	0.14
Crow's nest	0.12
Machinery:	
Ring mount with wind-direction servo mechanism	1.86
Machinery platform	0.62
Generator	1.24
Gearbox	1.76
V-belt drive and friction brake	0.12
Main shaft	0.72
Hub with blade bearings	0.39
Two blades	1.36
Pumps, control valves, power regulator and hydraulic lines	0.08
Fly weights with continuously adjustable gearbox and servomotor	0.22
Electrical lines, slipring set and current collector	0.15
Total weights	
Foundation	72.00
Guyed tubular tower	4.54
Machinery	8.52

Figure 4 shows the relationship between the wind velocity /335
averages and those for net power at the point of input into the utilities network. In this graph, 740 data selected as reliable are plotted from recorded 6-minute averages. The inclusion of a curve of statistical means in the area occupied by individual recordings was dispensed with, since the dispersion range, which is astonishingly narrow for measurements performed on wind power plants in a free stream of air, should remain immediately recognizable and, as a uniformly distributed band of points dispersed over the actual range, characterizes the operating states which are possible and are therefore to be expected.

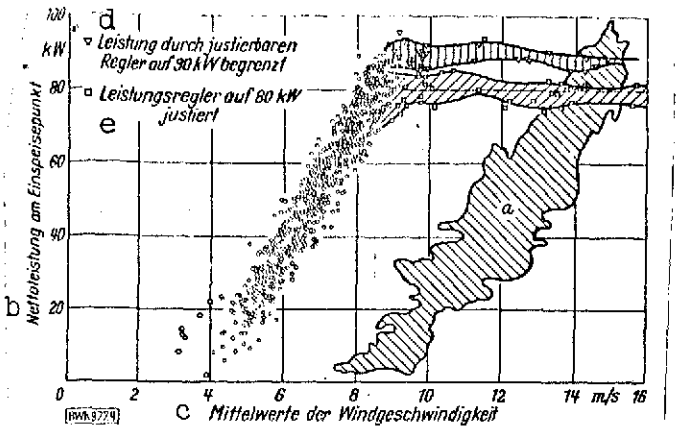

Fig. 4. Relationship between wind velocity and net power plant output: 740 measured values from tests, April to October 1961. The data points are 6-minute averages for net power at network input.

a. Range of dispersion for averages for the Andreau-Enfield-Cables plant, Algeria [3].

Key: b. Net power at network input point
c. Wind velocity averages
d. Power limited to 90 kW by adjustable regulator
e. Power regulator adjusted to 80 kW

The range of dispersion of output values for the 100-kW wind power plant constructed by Enfield-Cables, reported by F.H. Delafond [3], is included in the graph for comparison. This system weighed 60 t; the system of the Studiengesellschaft Windkraft weighed just a little over 13 t. The weight ratio of 1:4.5 probably corresponds roughly to the costs ratio. It is also notable that the system of the Studiengesellschaft Windkraft reaches maximum power as the Andreau plant is just beginning to produce.

The diagram also shows the regulatory behavior of the power plant in the velocity range above the wind velocities at which pre-set full load is reached. Its behavior is shown at two power-regulator settings (power limitation), at 80 and at 90 kW. We see that power is kept practically constant over a wide wind-velocity range, with a relatively small dispersion width.

Figure 5 compares the products, obtained from the recordings, of power coefficient and total efficiency ($c_p \eta_{tot}$) for the Studiengesellschaft Windkraft's power plant and the Andreau-Enfield-Cables power plant, plotted against the 6-min wind-velocity averages. The power coefficient is obtained from

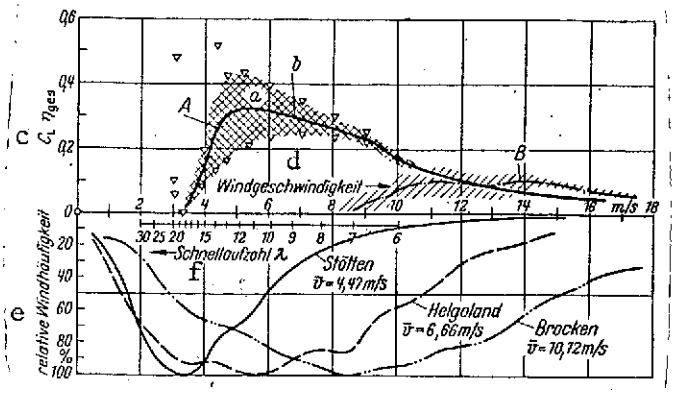

Fig. 5. Power coefficient × efficiency curves for the Stötten test power plant (A) and the Andreau-Enfield-Cables power plant (B) as functions of wind velocity.
a. Dispersion range of individual recordings; b. mean. Lower graph: typical examples of local relative wind frequencies.

Key: c. $c_p \eta_{tot}$
d. Wind velocity
e. Relative wind frequency
f. Speed ratio

$$c_P = \frac{P}{A_\varnothing} \cdot \frac{2}{\rho} \cdot \frac{1}{\bar{V}_o^3},$$

where

P = power delivered by rotor shaft

$A_\varnothing$ = effective circular area swept by blades

ρ = air density

V_o = wind velocity in undisturbed oncoming flow.

Conversion efficiency η_{tot} was determined as the product of individual efficiencies (Fig. 6, Table 4). Data provided by the supplying firms are used here for the generator and gearbox; the specified power requirements are used for the auxiliary drive equipment -- hydraulic pump, auxiliary pump drive system and power regulator. For the V-belt drive and for shaft-bearing losses, estimates were made such as those generally employed for these machinery elements. The relatively high transmission loss from the cable connection at the generator to the line connection at the transformer station for the 15 kV cross-country line results from the fact that the line cross section from the transformer to the instrument shed was originally designed only for the operation of a 10-kW plant.

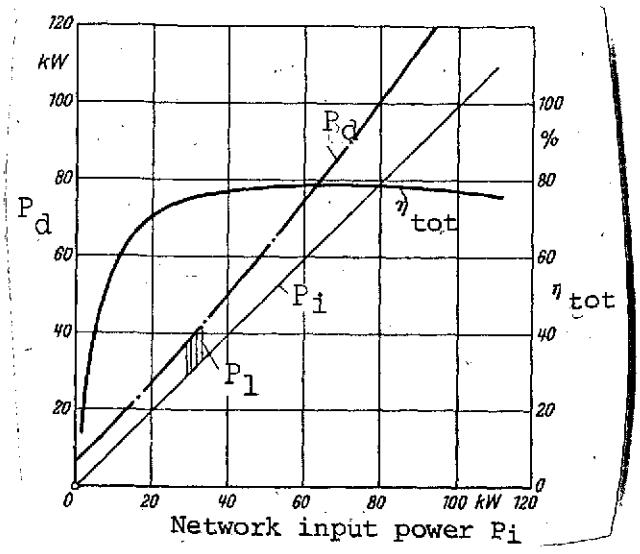

Fig. 6. Power P_d delivered by the rotor shaft and total conversion efficiency η_{tot} as functions of network input power P_i. Conversion power loss $P_l = P_d - P_i$.

TABLE 4. EFFICIENCIES OF POWER PLANT COMPONENTS AT VARIOUS OUTPUT LEVELS (REFERRED TO POWER DELIVERED TO NETWORK INPUT POINT).

$P_{delivered}$	$\eta_{generator}$	$\eta_{transmission}$	$\eta_{V\text{-belt}}$	$\eta_{oil\ pump,\ power\ regulator}$	$\eta_{transmission}$
kW	%	%	%	%	%
2	26	38	54	6	100
6	58	80	86	62	99,5
12	79,8	89	92	81	99
25	88	92,6	94,7	91	98
50	91,5	95,6	96,8	95,6	96
75	92	96,4	97,4	97,2	94
100	91	97,0	98,0	97,6	92
120	90	97,6	98,6	97,8	90

In addition to the typical examples shown in Fig. 5 for the curves of relative wind frequencies versus wind velocity, a scale is also plotted for the blade-tip speed ratios λ corresponding to the various wind velocities, but these apply only to the Studiengesellschaft Windkraft's plant.

The specific dispersion range of individual recorded data /336 is considerably larger at wind velocities below 6 m/s -- mean power below 40 kW -- than at wind velocities in the region of set nominal load. This results not only from the difference in wind structure at lower wind velocities but also from the power limitations of the machinery (high specific losses at low outputs, regulator control at high levels). The dropoff in the power coefficient - efficiency curve ($C_p\eta_{tot}$) can be clearly seen at the wind velocity at which the power regulator begins to respond. It is worth noting the comparison with the Andreau-Enfield-Cables power plant, which fares badly not only in absolute terms but also with respect to the wind frequency curves.

In order to be able to relate the results of output measurements to the precalculated rotor characteristic (Fig. 7), it was necessary to also take an average over the dispersion range of the individual 6-min measurements, using the conventional statistical methods, and to obtain the actual rotor-shaft power coefficients from the resultant power averages, as functions of wind velocity, taking the conversion power losses into consideration. The results of these computations are of very low reliability only in the region of extremely low power levels. This region is covered by many direct instantaneous-value observations, however (direct instantaneous measurement readings).

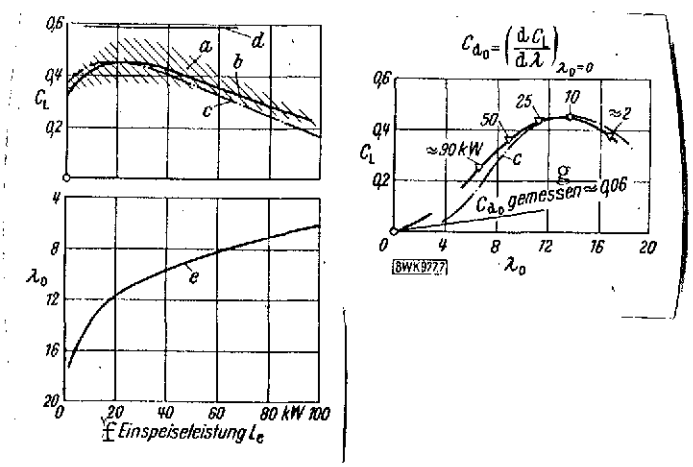

Fig. 7. Comparison of the characteristic calculated for the test power plant from 740 individual measurements of 6-min averages with the precalculated C_P/λ_0 graph (optimum blade angle).

C_L = effective rotor power coefficient C_P
λ_0 = speed ratio, referred to blade tip and undisturbed oncoming flow
a. Dispersion range of individual measurements
b. Measured data, 1960/61 (averages)
c. Precalculation, 1953
d. Theoretical optimum (no twist or friction)

[Key continued on following page.]

While idling, the power plant almost always remains on nominal rpm even at wind velocities below 3 m/s. Power levels above 6 kW could be taken from the rotor shaft here (see Fig. 6); the speed ratio was higher than 18.

The range of power levels above 60 kW is particularly well covered with a relatively small dispersion in individual measurements. At a power of 90 kW, the observed rotor power coefficient C_P is almost 50% higher than the

Key to Fig. 7, cont'd.:

e. Observed averages for speed ratios

Key: f. Network input power P_i
g. Measured

predicted value. This observation agrees with the results of back-calculating the startup torque coefficient from the necessary starting frictional torque of the power plant and the observed wind velocities at which the power plant begins to start up.

This behavior can be explained on the basis of the interactions between the high-arched, thick blade root profile (Göttingen 643 with thickness of 32% at a blade radius of 3 m) and the more outboard NACA laminar profiles of medium section thickness. The Göttingen profile has a shallow and "soft" $c_{a\ max}$ curve over the angle of attack. The propagation of regions of separated flow (which of course result in a decrease in the power coefficient at low speed ratios) in the inward direction, toward the blade root, is opposed by the powerful, sound flow in the area of small blade radii [4].

Thus from a blade root which has been carefully designed from the aerodynamic viewpoint, a supportive flow effect is also transmitted to blade areas located at a greater radius. With regard to energy output, this means that even when the optimum power coefficient was located in a region of relatively low absolute power (which is favorable for weak-wind behavior), the power output comes out better at relatively high wind velocities and power levels than for blades which are not optimally shaped in the root area.

Previously, the use of blade shapes which in aerodynamic terms were not ideal from such points of view had been necessary for production-engineering reasons, particularly in the case of very

large wind power plants. The manufacturing of blades of fiberglass-reinforced plastics provides almost unlimited freedom in blade configuration and thus makes it possible to meet all known aerodynamic requirements to a large degree [5-7].

In Fig. 8, the output plot (instantaneous values) and the recording strip from the Stötten Mountain Weather Station are /337
shown with the Weather Station's gust recording for August 31 and September 1, 1961. It is interesting here to compare the amplitude of fluctuations in instantaneous power and the amplitude of fluctuations in the 6-minute averages. Between 1:00 a.m. and 2:00 a.m., the fluctuations in instantaneous values amount to about ±30%, whereas the average fluctuations in successive 6-minute means exhibit a maximum of ±6% in this region. Even for a power plant which is independent of the network, this would mean that just a 6-minute storage unit would be sufficient to reduce the continual gust-induced power fluctuations to one fifth of the value which must be expected in operation without a storage unit.

Design and Configuration of the Fiberglass-Reinforced Blades

U. Hütter has developed a method for designing the blades which makes possible not only the prediction of rotor characteristics (power coefficient as a function of speed ratio, with the blade-setting angle as the parameter) and interpretation of the typical linearity of the power/wind-velocity relationship in the operating ranges of interest, but also the determination of blade stresses when loads are applied to the blades by strong and very strong gusts [4].

Corresponding to the conventions of aircraft construction, a number of defined cases of loading, so-called load cases, were assumed which in turn are broken down on the basis of the following:

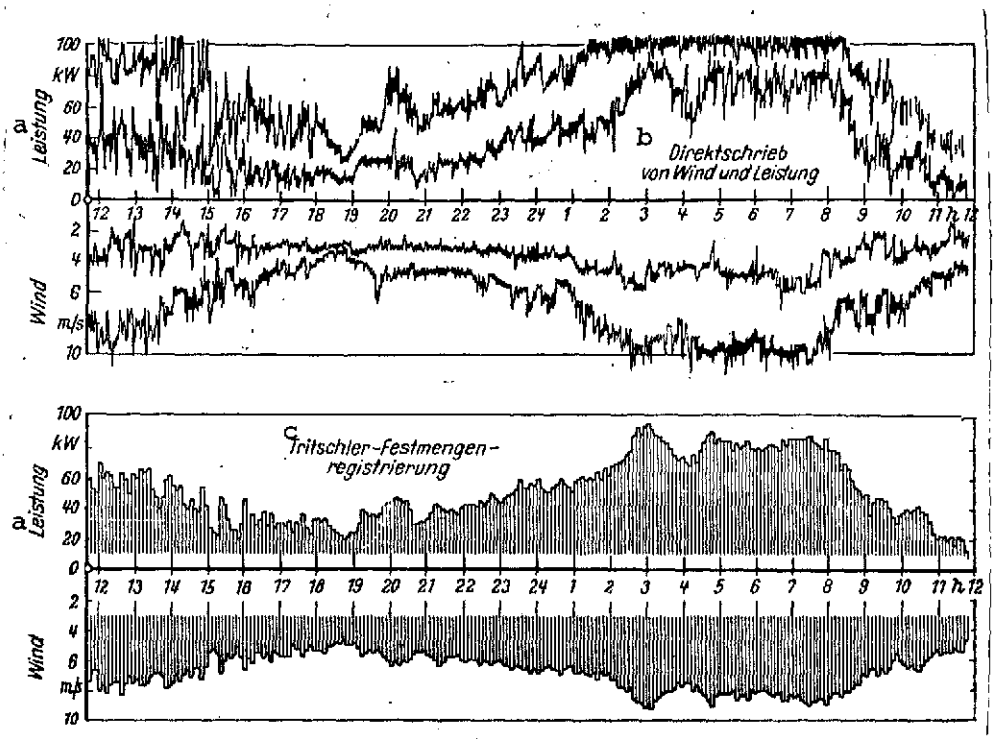

Fig. 8. Evaluation of continuous operation over a 24-hour period. Only the maximum and minimum values from the original recording are shown in the upper graphs.

Key: a. Power
b. Direct recording of wind and power
c. Tritschler fixed-quantity recording

H_1: especially infrequent load cases,

H_2: loads which occur occasionally but repeatedly in operation, and

H_3: loads which can be expected very frequently in continuous operation; in the most unfavorable case, at the frequency determined by rotor rpm.

In particular, blade dimensioning was based on the following load cases:

Load case 1a. With the power plant at a standstill and in the flat setting, i.e. with the blades in operating position, a

hurricane-like storm occurs with velocities of 60 m/s. The maximum value of the normal force coefficient $C_{n\ max}$ is reached over the entire blade here.

Load case 1b. As in case 1a, but the minimum value of the normal force coefficient $c_{n\ min}$ (i.e. the negative maximum of c_n) is reached over the entire blade.

For these load cases (H_1), a safety factor of j = 1.35 against reaching the yield point is provided for.

Load case 2a. The rotor operates at 2.5 times nominal load with blades in feathered position (position a in Fig. 9) and at the highest possible rpm under these conditions.

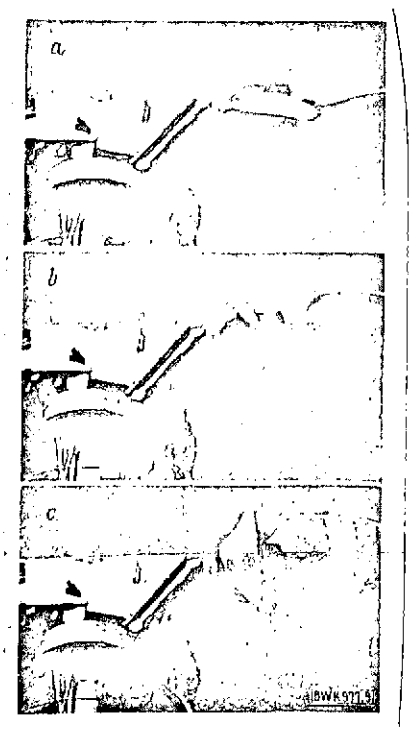

Fig. 9. The three most important blade settings.

a. Feathered position (no drive torque on rotor).
b. Intermediate position.
c. Optimum operating position.

This case likewise corresponds to H_1. It occurs if the blades are suddenly rotated by 70 to 90° without cutting out the generator from the network; j = 1.35 for reaching the yield point.

Load case 2b. Rotor turns at 2.5 times nominal load at a blade angle such that this power is absorbed by the rotor operating as a fan at nominal rpm. Corresponds to H_1; j = 1.35 for reaching the yield point.

Load case 3a. Average wind velocity sufficient for

reaching full load. System operates at nominal power. With the power plant operating at nominal rpm, wind velocity abruptly rises to twice the value of average wind velocity in a gust [20].

This load case must be expected very frequently (H_3). The safety factor must likewise be $j = 1.35$ for reaching fatigue-limit stresses ($2 \cdot 10^7$ load cycles).

Load case 3b. Average wind velocity sufficient to achieve full load. With power plant operating at nominal rpm, wind velocity abruptly dropped to $v_o = 0$ in a lull. Negative lifts suddenly occur on the blade. Air forces and centrifugal forces stress the blade in the same direction.

Loads corresponding to H_3; safety factor $j = 1.35$ for reaching fatigue-limit stresses ($2 \cdot 10^7$ load cycles).

In determining the stresses associated with load cases 3a and 3b, the loads are superimposed on those derived from the alternation of loads in the plane of rotation under the action of the blades' inherent weight.

Load case 4a. Average wind velocity is 2.5 times that at which nominal load is reached. The power plant is operating under a load. The blades are set to the point at which full power is just reached at 2.5 $v_{o\ \text{nom. load}}$. Wind velocity then increases abruptly in a gust to five times the value of $v_{o\ \text{nom. load}}$, the power plant reaching 10% overspeed.

This load case must occasionally be expected in operation (H_2). Safety factor $j = 1.35$ for reaching the "time strength" stresses (at 10^5 load cycles).

Load case 4b. In the same initial situation as in 4a, wind velocity drops to $v_o = 0$ in a lull. The "time strength" stress for 10^5 load cycles is reached at 10% overspeed with a safety factor of $j = 1.35$.

In load cases 4a and 4b, too, the alternating load in the plane of rotation resulting from the inherent weight of the blades is superimposed on the stresses which occur.

Load case 5. The rotor reaches 40% overspeed with the blades in the same setting as in load case 3a. Wind velocity abruptly drops to $v_o = 0$ in a lull. Safety factor $j = 1.35$ for reaching the yield point. This load case occurs occasionally in operation (H_2).

The studies of load cases have shown that cases 3a, 4a and 5 are decisive for the dimensioning of the blade, taking "time strength" and fatigue strength into consideration. Load case 1a, which produces the dominant loading in low-speed rotors and in high-speed rotors with speed ratios $\lambda < 4$, is not decisive for blade configuration in very-high-speed rotors.

U. Hütter has reported elsewhere on the method of production and on the aspects of materials selection and of processing -- fiberglass cords bonded with cold-setting resins (e.g. Palatal P6 polyester) [5]. See also [6-9] on the problem of the designing of fiberglass-reinforced plastic blades.

Within the scope of a Federal Ministry of Defense contract performed in the German Laboratory for Helicopters and Vertical-Flight Engineering (now Construction Methods Research Department of the DFL), measurements were made in 1962/63 on shells made of fiberglass-reinforced plastics with connecting flanges in a design like that of the blades on the 100-kW wind turbine, to determine

stress distribution within the shells, using embedded strain gauges. The shells were simultaneously subjected to bending moments and torques by means of a specially developed loading device, in a manner such as they occur during the application of stresses to rotor blades. These measurements provided indications that stress peaks can occur in the flange fillet under certain conditions, but that these remain within permissible limits when the flanges and counterstress rings are properly designed [10]. Particular attention is to be devoted to this situation as the tests are continued at the wind power plant at Stötten.

Control, Regulation, Automatic Cut-in Provisions

A report has been published [11] on the power plant's regulating system, from which the following material has been taken in part.

The blades are typical light weight components of high aerodynamic performance. All elements necessary for energy conversion, control and regulation have been incorporated into the machinery unit.

Specific power loading of the circular area swept by the blades is kept so low that even if the plant were set up on a site with a low average wind velocity, a particularly uniform energy output could be expected. Thus, in contrast to the designs of wind power plants of other working groups in France, Denmark, England, the U.S., etc., a design power of only 110 W/m^2 /338 was purposely selected instead of the specific installed power of 300 to 400 W/m^2 swept circular area generally found in those systems [1, 3, 15, 19].

The regulating system is designed in such a manner that the possibility exists of studying various regulating techniques and methods with respect to their practical usability during test operation.

The blade angles of the airfoils, which are designed to meet aerodynamic optimality requirements, are continuously adjustable, to meet operating requirements, via a large hydraulic servomotor. This servomotor operates at a system pressure of 12 to 20 technical atmospheres (gauge) against the action of aerodynamic and dynamic restoring torques in the blades and against a prestressed spring, the purpose of which is to rotate the blades to the feathered position[3] if the hydraulic system fails (Fig. 9).

Figure 10 shows the regulating circuit diagram. When left to itself in automatic operation, the system records wind velocity via anemometer a. As soon as the wind exceeds an average velocity of about 3 m/s over a metering interval (adjustable) of about 16 minutes, magnetic valve b is closed. The oil delivered by main pump c then no longer flows into oil tank d, but gradually begins to rotate the blades in the direction of the "operating setting" (setting c in Fig. 9). Control valve e initially assumes a position here which directs the oil coming from the pump into /339 hydraulic pressure line f, so that blades g are adjusted in the "higher rpm" direction.

The actuating linkage for the control valve is adjusted so that feedback lever h, which follows the blade setting, just returns the control valve to the center or floating position, via intermediate lever i, at the optimum blade setting. This occurs at a setting for power regulator k which tends to increase rpm.

The power regulator only ceases to command a higher rpm when the preset power level is reached. The rpm of the system thus initially increases until either speed regulator t or power regulator k begins to respond, and the blade setting is maintained or

[3]That blade position at which turbine-rotor drive torque vanishes ($\lambda \to 0$).

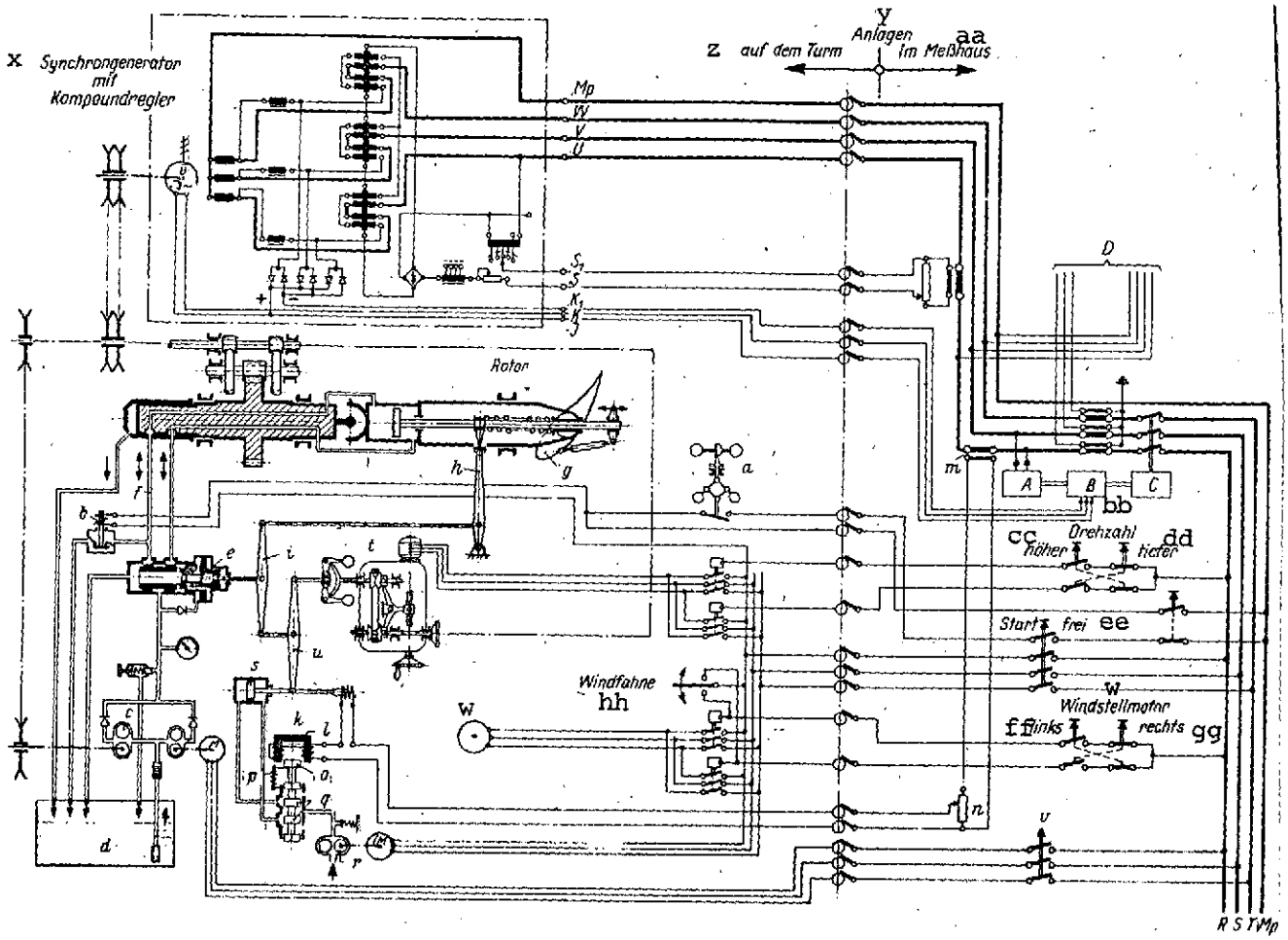

Fig. 10. Overall diagram of the control and regulating system.

A Cut-in sensor
B Excitation interruptor (and cut-in command)
C Main switch with overload and reverse-current protection
D Indicating and recording instruments

a Anemometer
b Magnetic valve
c Main oil pump
d Oil tank
e Control valve
f Hydraulic pressure line
g Blades
h Feedback
i Intermediate lever
k Power regulator
l Current coil
m Current transformer
n Sliding resistor
o Iron core
p Return spring
q Control pistons
r Servopump
s Actuating piston
t Speed regulator (flyweight)
u Cross bar
v Switch for auxiliary oil pump
w Wind servomotor
x Synchronous generator with compound regulator
y Systems
z On tower
aa In instrument shed
bb Rpm
cc Higher
dd Lower
ee Cleared to start
ff Left
gg Right
hh Wind indicator

shifted back via the control valve.

In parallel operation, regulation is accomplished only by means of the power regulator, and the speed regulator merely serves as an overspeed protector. Flyweight t is adjusted to a response rpm which is about 5% higher than nominal generator rpm in parallel operation, and thus responds only in case of overspeeding, e.g. in case of power network failure. The power limit, which can be adjusted between 30 and 120 kW at the regulator, is maintained in the test system with a precision of about ±5% (see Figs. 4 and 8).

Current coil l, which is linked via current transformer m with the primary current coming from the generator, serves as the primary sensing element for power regulator k. At nominal generator power, set by means of sliding resistor n, a current flows through the current coil which is just sufficient to attract iron core o against return spring p far enough that control pistons q are placed in the neutral position.

If generator current changes, the attractive force of current coil l likewise changes. The control pistons are shifted from the neutral position. The oil coming from servopump r consequently moves actuating piston s, and drive blades g are adjusted in the appropriate direction via control valve e: the greater the change in generator power, the more rapidly the adjustment is made.

During control functions via the power regulator (parallel operation), the pivot on the speed-regulator end of cross piece u serves as the fulcrum about which the power regulator actuates the cross piece and thus control valve e. If the flyweight in the speed regulator responds, the cross piece is moved about the pivot on the power-regulator end. By varying the transmission ratio

of the flyweight gearbox, it is possible to adjust generator speed between 250 and 1800 rpm.

Use can be made of these provisions in operation not connected with the power network if both rpm and power must be regulated. When the system is not connected with the public power supply, however, power can also only be kept constant via speed regulation, provided the power/rpm characteristic of the machinery to be driven has a sufficiently gentle slope. In order not to exceed a desired limiting rpm, the transmission ratio of the flyweight gearbox must be set to the corresponding value by hand or via the remotely controllable electric servomotor. The flyweight then begins to respond at the preset system rpm.

System startup by means of the AEG automatic cut-in unit proceeds as follows:

When a sufficient wind path (sufficiently high average wind velocity) has been recorded over an adjustable time period (adjustable from 1 to 30 min), magnetic valve b is closed. The blades are rotated toward a flatter position, and rpm increases if wind strength remains approximately constant. At about 90% of nominal rpm, the cut-in process is triggered by the voltage of the self-exciting generator, via a cut-in sensor. Excitation of the synchronous generator is temporarily interrupted, as a result of which generator voltage drops to about 20 V in approximately 1.5 s.

About 2.5 s later the generator, operating with its damper cage as an asynchronous machine, is cut in in parallel, with the suitably dimensioned choke coils absorbing the cut-in surge. After approximately 3 more seconds, excitation is again switched on and the choke coils bridged. During this 3 seconds, the generator is matched to the public power supply in frequency and phase and then operates synchronously while connected with it.

As long as the wind remains weak and the generator does not reach nominal power, the blades remain in the optimum operating position. If wind velocity increases, the adjusted nominal power, at which the power regulator begins to intervene, is reached at about 8 m/s.

When the power regulator responds, the blades are rotated via the hydraulic system to such a degree that the preset nominal power is not exceeded. The regulating range of the power regulator is so large that the preset power limit is not exceeded even at maximum wind velocity, due to slackening of the blade-setting angle.

If the wind drops off to such an extent that, in spite of the optimum blade setting, public power supply input is less than 5 kW for 3 s, the shutdown process is initiated. The generator is separated from the public power supply here, and magnetic valve b is opened. The blades are thereby returned to the starting position (corresponding approximately to setting b in Fig. 9). Wind recording is simultaneously resumed in order to prepare for a new cut-in process.

The system is also protected by several circuit breakers in the automatic parallel-switching and regulating equipment.

The shutdown process is immediately triggered in the following cases without automatic provisions for cutting in again:

1. Public power supply failure;
2. Failure of one phase;
3. Tripping of the generator overcurrent protection system;
4. Tripping of the overcurrent protection system at one of the electric motors, such as the wind servomotor, the servomotor on the power regulator, the positioning motor on the speed regulator, and the auxiliary oil pump motor;
5. Actuation of the speed regulator (overspeeding).

Magnetic valve b closes under tension, i.e. is opened automatically in case of public power supply failure, so the return spring in the main shaft returns the piston and thus the blades to the feathered position.

In case of failure or malfunction of the hydraulic system, too, this spring always acts on the blades in such a manner that they are returned to the starting position. At the optimum operating position, the return spring has a tension of about 2 Mg force on it, corresponding to an oil pressure of about 15 technical atmospheres (gauge) at the hydraulic servomotor.

For the sake of clarity, a simplified mode of representation was chosen for Fig. 8 [sic]. Details have been omitted such as the hazard shutdown system, additional circuit breakers, the generator de-energizing system and the automatic equipment for parallel operation, the various time-lag relays, the shutdown provision for less than 5 kW power, the operating schematic for wind recording, with start command, etc.

Rotation of the power plant into the wind is effected by a wind indicator vane via an electric motor and a worm gear. If the wind turns from the direction already set, the wind indicator switches on an electric motor in the appropriate direction, via a relay, and the machinery unit rotates until the wind indicator breaks contact because the vane is again in the direction of the wind.

A direct-acting aerodynamic/mechanical mechanism for adjust- /340
ing into the direction of the wind with the aid of a high-gear-ratio side wheel is also provided. A self-inhibiting differential gearbox is inserted ahead of the worm gear in the head of the tower for this purpose, which permits the optional use of the side wheel and/or servomotor in the adjustment process, without clutches.

REFERENCES

1. Gross, A.Th., "Using Wind Power in Europe? Results of the Yearly Meeting of the Studiengesellschaft Windkraft eV, Stuttgart," Brennst.-Wärme-Kraft 11(9), 414-419 (1959).

2. Clausnizer, G., Kurzzeitmessungen zur Bestimmung des Zusammenhanges zwischen Windgeschwindigkeit und Leistung einer Windkraftanlage [Short-Term Measurements to Determine the Relationship Between Wind Velocity and the Output of a Wind Power Plant], Dissertation, Karlsruhe Engineering College, 1959.

3. Delafond, F.H., "Testing Methods Used on the 100-kW Wind Generator," Report E/Conf. 35 W/9 for the United Nations Conference, Rome, 1961 (see also report in Brennst.-Wärme-Kraft 14(7), 309 ff., particularly 321-326 (1962).

4. Hütter, U., "The Aerodynamic Layout of Wing Blades of Wind-Turbines with High Tip-Speed Ratio," Report E/Conf. 35/W/31 for the United Nations Conference, Rome, 1961.

5. --, "Load-Bearing Aircraft Components Made of Fiberglass-Reinforced Plastics," Luftfahrttechn. 6(2), 34-44 (1960).

6. --, "Highly Stressed Light Weight Components Made of Fiberglass-Reinforced Plastics," Kunststoffe 50(6), 318-324 (1960).

7. --, "Propellers and Helicopter Rotor Blades Made of Fiber-Reinforced Synthetic Resins," Jahrbuch 1960 der Wiss. Ges. für Luftfahrt eV [1960 Yearbook of the Scientific Society for Aeronautics], Braunschweig, 1961, pp. 374-381.

8. --, "Glass-Fiber Reinforced Plastics as Structural Material for the Aircraft Industry," Society of the Plastics Industry, Inc., Technical and Management Conference, Reinforced Plastics Division, 16th Annual, Section 13-A, Chicago, 1961.

9. --, "The Transfer of Force in Highly Stressed Monocoque Bodies of Glass-Reinforced Plastics," Plast. Inst. Trans. J., 16-27 (1962).

10. --, "Measurement of Three-Dimensional Stress States with Embedded Strain Gauges in Glass/Resin Structures," Kunststoffe 53(11), 831-838 (1963).

11. Armbrust, S., "Regulating and Control System of an Experimental 100-kW Wind Electric Plant Operating Parallel with an AC Network," Report E/Conf. 35/W/34, for United Nations Conference, Rome, 1961.

12. Betz, A., Wind-Energie und ihre Ausnützung durch Windmühlen [Wind Energy and Its Utilization by Windmills], Göttingen, Vandenhoeck u. Ruprecht, 1926.

13. Hütter, U., "The Effect of Wind Frequency on the Determination of Wind Power Plant Speeds," Z. Elektrotechn. 1(6), 117-122 (1948) and 2(1), 10-15 (1949).

14. Clausnizer, G., "Operation of an 8.8-kW Wind Power Plant in Parallel with a Power Supply Network," Report No. 1 of the Studiengesellschaft Windkraft eV, Stuttgart, 1953.

15. Juul, J., "Report on Results Attained with the Experimental Windmill of Sydstjaellands elektrizitets Aktieselskab (SAES)," Meeting of the Committee for Productivity and Applied Research (PRA), Working Party No. 2, OEEC, London, 1950.

16. Strscheletzky, M., Hydrodynamische Grundlagen zur Berechnung der Schiffsschrauben [Hydrodynamic Principles for Ship-Propeller Calculations], Karlsruhe, G. Braun, 1950.

17. Weinig, F., Aerodynamik der Luftschraube [Propeller Aerodynamics], Berlin/Göttingen/Heidelberg, Springer Verlag, 1950, p. 139 ff.

18. Hoerner, S.F., Aerodynamic Drag, Dayton, Ohio, The Otterbein Press, 1951.

19. Sabinin, G.A., Theorie schnellaufender stabilisierter Windräder [Theory of Stabilized High-Speed Wind Wheels], TsAGI [N.Ye. Zhukovskiy Central Institute of Aerohydrodynamics], Office of Scientific Information edition, 1953 (Russian), pp. 16-20.

20. Robitzsch, M., "Information Concerning the Structure of Ground Wind," Lindberger Jahrbuch [Lindberg Yearbook], Vol. 13, 1919, p. 66 ff.